Adsorption Kinetics of the Ionic Surfactant Decanoic Acid

Alvin Casandra,[a] Ya-Chi Lin,[a] Libero Liggieri,[b] Ruey-Yug Tsay,[c*] and Shi-Yow Lin[a]*

[a] Department of Chemical Engineering, National Taiwan University of Science and Technology, 43 Keelung Road, Sec. 4, Taipei, 106 Taiwan

[b] CNR - Istituto per l'Energetica e le Interfasi IENI - UOS Genova, via De Marini, 6 Genova, Italy

[c] Institute of Biomedical Engineering, National Yang-Ming University, 155 Li-Nung St., Sec.2, Taipei, 112 Taiwan

*Author to whom correspondence should be addressed.

E-mail: tsay@ym.edu.tw and sylin@mail.ntust.edu.tw

Graphical Abstract

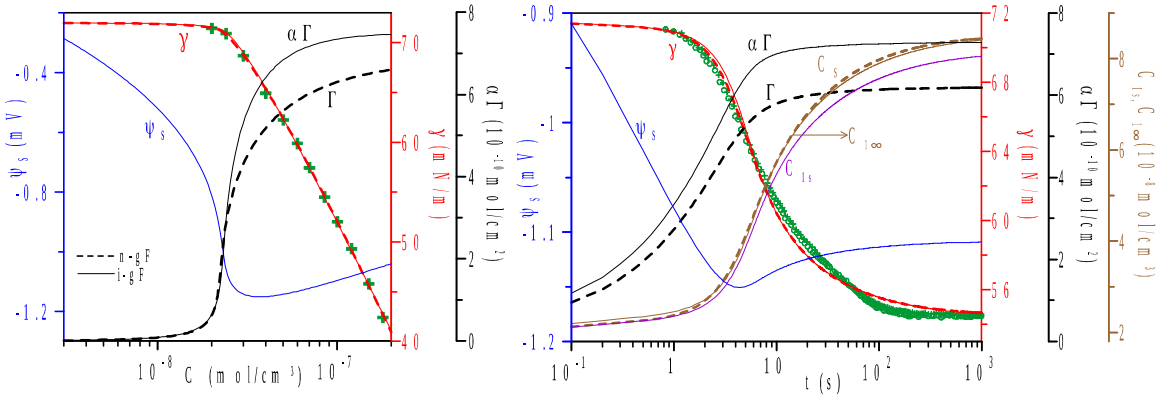

Highlights

- Dynamic/equilibrium surface tensions of decanoic acid solutions were measured.
- Complete sets of ST relaxation curves were obtained using a pendant bubble tensiometer.
- The ionic generalized Frumkin model describes the ST relaxation data very well.
- A diffusivity of 5.5×10^{-6} cm^2/s was determined from the dynamic surface tension data.
- Relaxation of the surface/sublayer properties [Γ, ψ_s, C_{1s}, C_1 , $\psi(r)$ and (t)] was reported.

Adsorption Kinetics of the Ionic Surfactant Decanoic Acid

Alvin Casandra,[a] Ya-Chi Lin,[a] Libero Liggieri,[b] Ruey-Yug Tsay,[c*] and Shi-Yow Lin[a]*

[a] Department of Chemical Engineering, National Taiwan University of Science and Technology, 43 Keelung Road, Sec. 4, Taipei, 106 Taiwan

[b] CNR - Istituto per l'Energetica e le Interfasi IENI - UOS Genova, via De Marini, 6 Genova, Italy

[c] Institute of Biomedical Engineering, National Yang-Ming University, 155 Li-Nung St., Sec.2, Taipei, 112 Taiwan

Abstract

The adsorption kinetics of ionic surfactant decanoic acid was examined. Dynamic and equilibrium surface tensions (ST) were measured using a video-enhanced pendant bubble tensiometer. The equilibrium ST data and the complete ST relaxation profiles were compared with theoretical profiles predicted by both non-ionic and ionic models. The quasi-equilibrium approach was used in the ionic model to describe the electric field in the electrical double layer. Both non-ionic and ionic generalized-Frumkin models predict the equilibrium and dynamic ST data very well. Using the ionic model, a comparison between the dynamic ST data and the theoretical ST profiles gave a diffusivity of 5.5×10^{-6} cm^2/s. The adsorption of decanoic acid onto the air-water interface was determined to be diffusion controlled. Dynamic surface properties (Γ and ψ_s), the electrical potenial $\psi(r, t)$ in the double layer, and the double layer thickness $\lambda(C, t)$ were also evaluated. It was found that the surface charge density increases very quickly at the early stages (~1 s) of the surfactant adsorption process. Additionally, the electrical surface potential data implied that the surface charge density becomes significantly stronger at very dilute surfactant concentrations, where π is less than 1 mN/m.

Keywords: adsorption kinetics; ionic surfactant; dynamic surface tension; diffusion coefficient; decanoic acid

*Author to whom correspondence should be addressed.

E-mail: tsay@ym.edu.tw and sylin@mail.ntust.edu.tw

1. Introduction

Surfactant molecules are commonly used for reducing the surface tension of liquid-gas interfaces in industrial processes [1], including sundry practical applications and products like detergents, inks, adhesives, pesticides, cosmetics, among others [2]. Since the optimal dosage of a surfactant relies on specific knowledge of dynamic adsorption properties [3], it is not surprising that investigations on the kinetics of surfactant adsorption have gained tremendous interest in the past two decades.

Surfactants are amphiphilic molecules that commonly have a simple structure consisting of a hydrocarbon chain bound with a hydrophilic head group. Surfactant monomers are sparingly soluble in an aqueous phase because of the unfavourable interactions between the surfactant hydrocarbon chain and water. These unfavourable interactions make surfactant molecules preferentially adsorb at the air-water interface, which depletes the surfactant concentration in the sublayer and initiates the surfactant adsorption process [4] once a fresh air-water interface has been created. For ionic surfactants, a surface charge density is established as a result of the adsorption of ionic surfactant molecules. This surface-charge density creates a repulsive force in the electrical double layer and significantly affects the mass transport of ionic surfactant molecules. The surfactant adsorption process consists of at least three steps: bulk diffusion, adsorption-desorption between the subsurface, and surface re-arrangement. In this study, a pendant bubble was formed in a static uniform aqueous solution of ionic surfactants with nearly negligible convection [5].

There are approximately ten articles in the literature that have reported dynamic surface tension (ST) data for ionic surfactants in the past decade [6-17]. However, only three of these articles give complete dynamic ST profiles (from the ST of the solvent to its equilibrium value). Datwani and Stebe [6] applied a pendant bubble method to measure an aqueous Aerosol-OT solution with 10–500 mM NaCl and several complete sets of dynamic ST curves were obtained. Then, an ionic Langmuir model was used to simulate the surfactant adsorption process. Stubenrauch et al. [7] and Mucic et al. [8] applied the maximum bubble (or drop) pressure method for C_nTAB (n=14 and 16) solutions and 3–5 complete sets of dynamic ST curves for each surfactant were obtained. In this case, the authors applied a Frumkin ionic compressibility model for simulating the adsorption process.

Several other articles have also reported some dynamic ST data [9-17]. Unfortunately, these dynamic ST data excluded the initial portions of the ST curves. This data loss is because of the high

surfactant concentration and the lack of a suitable instrument for measuring the initial relaxation phase of the ST process (usually at t <1 s). In these studies, the long time approximation model of nonionic surfactants was commonly applied for simulating the surfactant adsorption process.

To the best of our knowledge, there are only three articles in the past decade that have showed the dynamic ST data of ionic surfactants without the addition of salt or buffer [7, 9, 17]: cationic surfactant C_nTAB by Stubenrauch et al. [7], catanionic alkyltrimethylammonium decanoate by Li et al. [9], and anionic oxyethylated surfactant by Miller [17]. However, only one of these reports [7] provided a complete ST relaxation profile.

Davies and Rideal [18] proposed an ionic Langmuir adsorption isotherm in 1963. Dukhin et al. [19-21] introduced the idea of a quasi-equilibrium approach by using Gouy-Chapman theory [22, 23], which relates the surface charge density and the surface potential in an electrical double layer. This quasi-equilibrium model was then frequently applied to the study of adsorption kinetics of ionic surfactants [24-27]. In 1994, MacLeod and Radke [28] compared the difference between the quasi-equilibrium approach and the full transient model (i.e., the Nernst-Plank diffusion equation). They concluded that the difference between these models occurs only at times inaccessible to current dynamic surface tension techniques.

The aim of this study is to investigate the adsorption kinetics of decanoic acid without salt. A video-enhanced pendant bubble tensiometer was employed for the dynamic/equilibrium ST measurement. A comparison between the experimental data (i.e., a complete set of ST curves) and theoretical ST profiles predicted from an ionic Frumkin model was performed. Moreover, the relaxation of surface properties and the distribution of the ionic surfactant in the electrical double layer were reported. An outline of this paper is as follow: Section 2 describes briefly the pendant bubble experimental method. The theoretical framework for surfactant mass transport is detailed in section 3. In section 4, the experimental dynamic ST data are compared with the theoretical ST profiles from the ionic model. The paper concludes in section 5 with a discussion.

2. Experimental measurements

Materials. Decanoic acid ($C_{10}H_{21}COOH$, M.W. = 172.26 g/mol), purchased from Fluka Chemical (GC grade, purity ≥99.5%), was used without modification. Acetone (HPLC grade), which was used to calibrate the surface tension measurement, was obtained from Fisher Scientific Co. The water with which the aqueous solutions were prepared was purified via a Barnstead

NANOpure water purification system, with the output water having a specific conductance of less than 0.057 μS/cm. The values of the surface tension of air-water and air-acetone using the pendant bubble technique described in the following sections were 72.0 mN/m and 23.1 mN/m, respectively, at 25.0°C.

Tensiometer. A video-enhanced pendant (emerging) bubble tensiometer was employed for the measurement of the equilibrium (γ(C)) and dynamic (γ(t)) surface tension of the aqueous decanoic acid solutions at 25.0± 0.1°C. The apparatus (shown in Figure 1) and the edge detection routine have been described in detail in a previous study [5]. The temperature variation of the aqueous solution was less than ±0.1 K during the measurement of γ(t). A 16-gauge stainless steel inverted needle (0.047 in. I.D.; 0.065 in. O.D.) was used to generate the bubble.

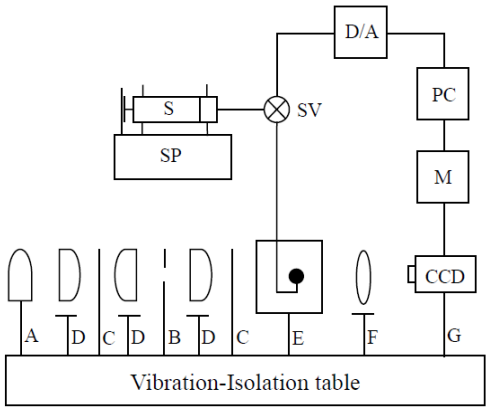

Figure 1. A pendant bubble apparatus and the video image digitization equipment. A: light source; B: pinhole; C: filter; D: planoconvex lens; E: quartz sample cell and inverted needle inside thermostatic air chamber; F: objective lens; G: video camera; M: monitor; PC: personal computer; D/A: data translation card; S: syringe; SP: syringe pump; SV: solenoid valve.

Measurement. A pendant bubble of air with a diameter of approximately 2 mm was formed in a decanoic acid solution, which was put in a quartz cell. Digital images of the bubble were taken sequentially and were processed to determine the edge coordinates. The edge coordinates of the pendant bubble were fitted to the theoretical bubble profiles generated from the classical Young-Laplace equation to obtain the surface tension. In this work, the time required to create an air bubble is approximately 0.72 seconds.

The measurements were taken for several different bulk concentrations: 2.0–18.0 (10^{-8} mol/cm^3). Each sample was performed in duplicate. Bubbles were measured for up to 1 or 2 h, depending on the surfactant concentration, to ensure that γ(t) reached its equilibrium value. The accuracy and reproducibility of the surface tension measurements obtained by this procedure are

approximately 0.1 mN/m [5]. A pH meter (MP8100, AI-ON Industrial Corp., Taiwan) was used to measure the pH values of the decanoic acid solutions at 25.0°C

3. Theoretical Framework

Mass transport. The mass transport of surfactant molecules onto a freshly created surface in a quiescent solution was modeled. Presently, only the case of one-dimensional diffusion and the adsorption onto a spherical interface from a bulk phase containing an initially uniform concentration of decanoic acid was considered. The surfactant molecules were assumed not to dissolve into the gas phase of the pendant bubble.

Dukhin et al. [19-21] developed a quasi-equilibrium approach for the diffusive transport of ionic surfactants with an assumption. That is, the double-layer potential is always in an instantaneous quasi-equilibrium with the concentration at the double-layer boundary. MacLeod and Radke [28] compared the solutions from this quasi-equilibrium approach to those from the Nernst-Planck diffusion equation by solving the coupled Nernst-Planck and Poisson equations in the bulk phase. They concluded that the difference between the full transient model and the quasi-equilibrium approach occurs only at times inaccessible to current dynamic surface tension techniques.

The quasi-equilibrium model was adopted in this study. The diffusion of the surfactant in the bulk phase can be described by Fick's law [29]:

$$\frac{\partial \mathrm{C}}{\partial \mathrm{t}} = \frac{\mathrm{D}}{\mathrm{r}^2}\frac{\partial}{\partial \mathrm{r}}\left(\mathrm{r}^2 \frac{\partial \mathrm{C}}{\partial \mathrm{r}}\right) \tag{1}$$

with initial and boundary conditions

$$C(r > \lambda, t = 0) = C_0 \tag{2a}$$

$$\Gamma(t = 0) = 0 \tag{2b}$$

$$C(r \to \infty, t > 0) = C_0 \tag{2c}$$

$$\frac{\mathrm{d}\Gamma(\mathrm{t})}{\mathrm{dt}} = \mathrm{D}\frac{\partial \mathrm{C}}{\partial \mathrm{r}}\bigg|_{r=b} \tag{2d}$$

where λ is the characteristic length of the double-layer, b is the radius of the pendant bubble at the apex (Figure 2), C is the surfactant concentration in the bulk phase, C_0 is the initial bulk concentration, D is the surfactant diffusivity, and Γ is the surfactant surface concentration. The boundary condition (2d) indicates that the adsorption rate of surfactant molecules at the surface is equal to the diffusion rate of surfactant molecules from bulk phase to the subsurface because the

sublayer has zero volume.

By using the Laplace transform, the above set of equations can be solved in terms of the unknown subsurface concentration $C_S(t) = C(r=b, t)$ [5]:

$$\Gamma(t) = \Gamma_b + (D/b)\left[C_0 t - \int_0^t C_S(\tau)\right] + 2(D/\pi)^{1/2}\left[C_0 t^{1/2} - \int_0^{\sqrt{t}} C_S(t-\tau)\, d\tau^{1/2}\right] \qquad (3)$$

where Γ_b is the initial surface concentration and is equal to zero for a fresh interface. Note that for ionic models, the subsurface concentration is $C_S = C_{1\infty}$, where $C_{1\infty}$ is the surfactant concentration at the outer electric double layer. The above expression is the spherical surface analogue of Ward and Tordai's result for the diffusion toward a planar surface [30].

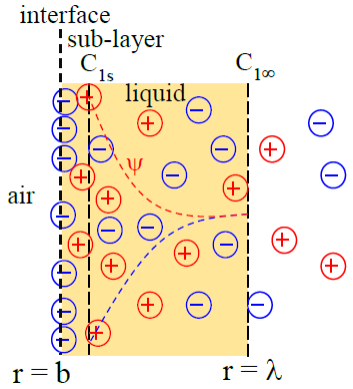

Figure 2. Schematic diagram of the double-layer. λ is the characteristic length of the double-layer, C_{1s} is the surfactant concentration at the sublayer, $C_{1\infty}$ is the surfactant concentration at the outer double layer, and b is the radius of the spherical bubble.

To complete the solution for the surface concentration (Γ), the sorption kinetics must be specified. The adsorption model used here assumes that both adsorption and desorption are activated processes:

$$\frac{d\Gamma}{dt} = \beta \exp\frac{-E_a}{RT} C_{1s}[\Gamma_\infty - \Gamma(t)] - \alpha \exp\frac{-E_d}{RT}\Gamma(t) \qquad (4)$$

where C_{1s} is the surfactant concentration adjacent to the interface, E_a and E_d are the activation energies for the adsorption and desorption processes, respectively, and β and α are the pre-exponential factors for the adsorption and desorption processes, respectively. The activation energies were assumed to be surface concentration dependent with the following power law relationship:

$$E_a = E_a^0 + \nu_a \Gamma^n \qquad (5a)$$

$$E_d = E_d^0 + \nu_d \Gamma^n \qquad (5b)$$

The diffusion flux established a concentration relationship between the inner (C_{1s}) and outer ($C_{1\infty}$) sublayer of the electric double layer by an instantaneous Boltzmann distribution [31, 32]:

$$C_{1s} = C_{1\infty} \exp\left(\frac{-z_1 F\psi_s}{RT}\right) \tag{6}$$

where F is Faraday's constant, R is the ideal gas constant, T is the absolute temperature, Ψ_s is the electrostatic potential at the interface and z_1 is the surfactant charge. From equations 4–6, the adsorption equation becomes:

$$\frac{d\Gamma}{dt} = \beta^* \exp\frac{-\upsilon_a \Gamma^n}{RT} \exp\left(\frac{-z_1 F\psi_s}{RT}\right) C_{1\infty}[\Gamma_\infty - \Gamma(t)] - \alpha^* \exp\frac{-\upsilon_d \Gamma^n}{RT} \Gamma(t) \tag{7}$$

where $\beta^* = \beta \exp(-E_a^0/RT)$, $\alpha^* = \alpha \exp(-E_d^0/RT)$, E_a^0, E_d^0, ν_a, and ν_d are constant.

At equilibrium, the rate of change of the surface concentration at the interface (Γ) with time vanishes, and the adsorption isotherm becomes:

$$\frac{\Gamma}{\Gamma_\infty} = x = \frac{C_{1\infty}}{C_{1\infty} + a\exp(Kx^n + \frac{z_1 F\psi_s}{RT})} \tag{8}$$

where Γ_∞, K, a and n are the four model parameters of the generalized-Frumkin isotherm, and x is the dimensionless concentration. The parameter K considers the molecular interactions among the adsorbed surfactants and "a" indicates the surfactant activity. Equation 8 becomes the popular ionic Frumkin isotherm [33, 34] when $n = 1$. The equation becomes the non-ionic model when $z_1=0$.

In this model, Gouy-Chapman theory was utilized to describe the screening of the surface charge and the correlation between the surface charge density and the electrical potential in the double layer [23, 24]. Brownian motion of the ions in solution introduces a certain degree of chaos, causing the ions to be dispersed in the region of the charged surface. This phenomenon forms a "diffuse" double layer in which the local ion concentration is determined by eq. 6 [32]. The electrical potential (Ψ) is therefore determined by the nonlinear Poisson-Boltzmann equation [31, 35]:

$$\nabla^2\psi = -\sum_i \frac{z_i C_{i\infty} F}{\varepsilon} \exp\left(\frac{-z_i F\psi}{RT}\right) \tag{9}$$

where ε is the permittivity of the medium. At the interface (r=b), $\Psi = \Psi_s$. When there is no additional salt or only one single salt is added in the surfactant solution, eq. 9 can be further simplified to [35]:

$$(\nabla\psi)_{r=b} = -2\left(\sum_i \frac{C_{i\infty} RT}{\varepsilon}\right)^{1/2} \sinh\left(\frac{-z_1 F\psi_s}{2RT}\right) \tag{10}$$

The adsorption of ionic surfactant molecules onto the interface results in an increase of the surface charge density (σ) [19, 35]:

$$\sigma(t) = \sigma_0 + z_1 F \Gamma(t) \tag{11}$$

where σ_0 is the initial surface charge density at the interface and $z_1F\,\Gamma(t)$ describes the increase in the surface charge density caused by the surfactant adsorption. In this work, $\sigma_0 = 0$ because there is zero surface charge density at the fresh air-water interface (i.e., at t = 0). The surface charge density dictates the potential gradient at the interface [36]:

$$\frac{\sigma(t)}{\varepsilon} = -\left(\nabla \psi\right)_{r=b} \tag{12}$$

Therefore, the relationship between the surface charge density ($z_1F\,\Gamma$) and the electrical potential at the interface (Ψ_s) is given by [35]:

$$\frac{z_1 F \Gamma}{\varepsilon} = 2\left(\sum_i \frac{C_{i\infty} RT}{\varepsilon}\right)^{1/2} \sinh\left(\frac{z_1 F \psi_s}{2RT}\right) \tag{13}$$

Numerical solution. The Gibbs adsorption equation $d\gamma = -\alpha\Gamma RT\, d\ln C$ (where α indicates the dissociation degree) and the equilibrium isotherm (eq. 8) permit calculation of the surface tension for ideal solutions [34]:

$$\gamma = \gamma_0 + \alpha RT\Gamma_\infty[\ln(1-\frac{\Gamma}{\Gamma_\infty}) + \frac{Kn}{(n+1)}(\frac{\Gamma}{\Gamma_\infty})^{n+1}] - \gamma_{el} \tag{14}$$

Note that $\alpha=1$ for non-ionic surfactants, $\alpha= 2$ for ionic surfactants, and $1< \alpha < 2$ for decanoic acid because of its partial ion dissociation, which is concentration dependent.

The effect of decreasing surface tension via electrostatic repulsion is significant for ionic surfactant solutions. An equation of state considers both the surface tension decrease from the surface concentration and the surface potential (i.e., a surface excess Maxwell stress). The equation of state for an ionic surfactant becomes [36]:

$$\gamma = \gamma_0 + \alpha RT\Gamma_\infty[\ln(1-\frac{\Gamma}{\Gamma_\infty}) - \frac{Kn}{(n+1)}(\frac{\Gamma}{\Gamma_\infty})^{n+1}] - \frac{4RT}{z_1F}(2\varepsilon RTC_{1\infty})^{1/2}\ [1-\cosh(\frac{z_1F\psi_s}{2RT})] \tag{15}$$

When the adsorption process was controlled solely by bulk diffusion, the surface concentration (Γ) and chemical potential at the interface (Ψ_s) can be obtained by solving the bulk diffusion equation (eq. 3, which describes the mass transport between the bulk solution and the sub-layer), the adsorption isotherm (eq. 8, which describes the mass transport between the sub-layer and the interface) and the surface potential equation (eq. 13). If the adsorption was controlled in a diverse

manner, the adsorption kinetics equation (eq. 7) was used instead of the adsorption isotherm (eq. 8) to describe the adsorption-desorption process between the sub-layer and the interface. In this study, an ODE package in Matlab was used to solve these three equations simultaneously (i.e., either eqs. 3, 8 and 13 or eqs. 3, 7 and 13). The dynamic surface tension γ(t) was calculated from the equation of state (eq. 15) once both Γ and Ψ_s were known.

4. Results

Surface Tension. The relaxation of the surface tension γ(t) for the adsorption of decanoic acid onto a clean air-water interface was measured up to 1–2 h from the moment (referenced as t=0) at which one-half of the bubble volume was generated during the bubble formation at 25.0 ± 0.1°C. Shown in Figure 3 are representative γ(t) profiles (for one selected bubble at each concentration) of decanoic acid solutions at 12 different concentrations. The equilibrium surface tension was extracted from the long-time asymptotes in Figure 3 and plotted as the symbol in Figure 4.

Model determination. Figure 4 shows the comparison between the equilibrium ST data of decanoic acid and the best fit from the adsorption isotherms of nonionic Langmuir, nonionic Frumkin, nonionic generalized-Frumkin, ionic Langmuir, ionic Frumkin, and ionic generalized-Frumkin models. The constants of the model (listed in Table 1) were obtained by adjustment to minimize the error between the model predictions and the experimental equilibrium tension data.

Both the Frumkin and generalized Frumkin models predict a maximum surface concentration of approximately 6.6–7.6 (10^{-10} mol/cm^2) for decanoic acid at the air-water interface. The corresponding surface area occupied per surfactant molecules (A) is approximately 22–25 Å^2/molecule. This A value is consistent with the data (22.6 A^2/molecules) reported by Lunkenheimer et al. [37] for n-alkanoic acid (carbon number = 6–11), which was measured via an analysis of its crystal structure. Further, this A value indicates that decanoic acid molecules are well packed at the air-water interface.

Both Frumkin isotherms (n-F and i-F) predict the equilibrium γ(C) data well at γ< 65 mN/m. However, a significant deviation exists for the Frumkin models at low surface pressure (γ> 65 mN/m). It is noteworthy that the nonionic Frumkin isotherm is more predictive than the ionic Frumkin model. A more significant error was observed for both Langmuir models (n-L and i-L) for the entire γ(C) range. Both generalized Frumkin isotherms (n-gF and i-gF) predict the equilibrium γ(C) data much better that the Frumkin isotherms. It is noted that the nonionic generalized-Frumkin

isotherm predicts the equilibrium γ(C) data as well as the ionic generalized-Frumkin isotherm. Both Langmuir isotherms poorly predict the equilibrium γ(C) data.

Dynamic ST. If the adsorption of decanoic acid onto a clean interface was assumed to be diffusion controlled, the dynamic ST data (in Figure 3) can be used to determine the diffusivity of decanoic acid molecules in the aqueous phase. The model constants listed in Table 1 were used for the dynamic ST calculations.

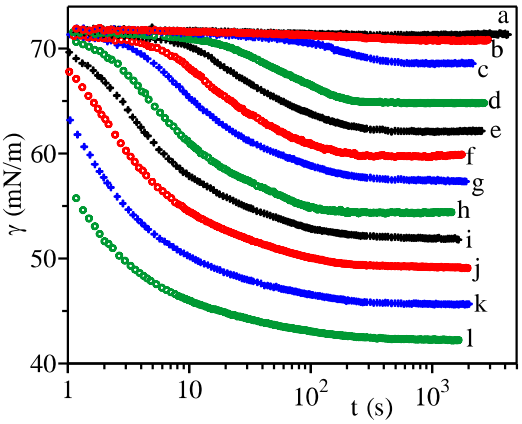

Figure 3. Relaxations of surface tension of aqueous decanoic acid solutions at various bulk concentrations: C = 2.0 (a), 2.4 (b), 3.0 (c), 4.0 (d), 5.0 (e), 6.0 (f), 7.0 (g), 8.5 (h), 10.0 (i), 12.0 (j), 15.0 (k), and 18.0 (l) (10^{-8} mol/cm^3).

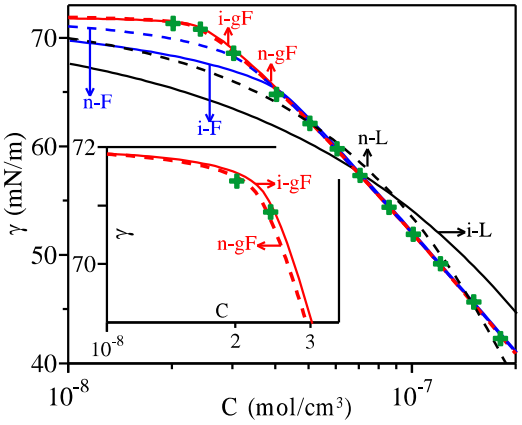

Figure 4. Equilibrium surface tension of aqueous decanoic acid solutions and the theoretical predictions of nonionic (dashed curves) and ionic (solid curves) models. Model constants are listed in Table 1.

Both Frumkin models (n-F and i-F) predict well the dynamic ST at γ(t)< 65 mN/m. However, poor predictive behavior was observed at γ(t)> 65 mN/m (Figure 5). This poor prediction at γ(t)> 65 mN/m matched these models poor prediction for the equilibrium ST data, as shown in Figure 4. Both generalized Frumkin models predict well the dynamic ST data. However, different values of diffusivities were obtained from fitting the dynamic ST data: 5.5 and 12.0 (10^{-6} cm^2/s) for

the ionic-gF and nonionic-gF models, respectively. It is noted that using the i-F and n-F models to fit the dynamic ST data resulted in similar diffusivities: D= 6.0 and 12.0 (10^{-6} cm^2/s) for the i-F and n-F models, respectively

Table 1. Model constants for aqueous decanoic acid solutions

model[¶]	$\alpha\Gamma_\infty$ (10^{10} mol/cm^2)	a (mol/cm^3)	K	n	K/K_c[§]
n-L	34.86	4.18×10^{-7}	-	-	-
n-F	6.669	1.89×10^{-7}	-3.579	1	0.89
n-GF	6.861	4.70×10^{-6}	-6.393	0.295	0.94
i-L	17.73	1.29×10^{-12}	-	-	-
i-F	7.599	5.80×10^{-12}	-7.100	1	0.95
i-gF	7.507	6.08×10^{-3}	-27.72	0.138	0.94

[¶] L = Langmuir; F = Frumkin; gF = generalized-Frumkin; n- = non-ionic model; i-= ionic model.

[§] K_c = Critical K value: $K_c = -(1+1/n)^{1+n}$ for nonionic models, K_c for ionic models (Figure 11).

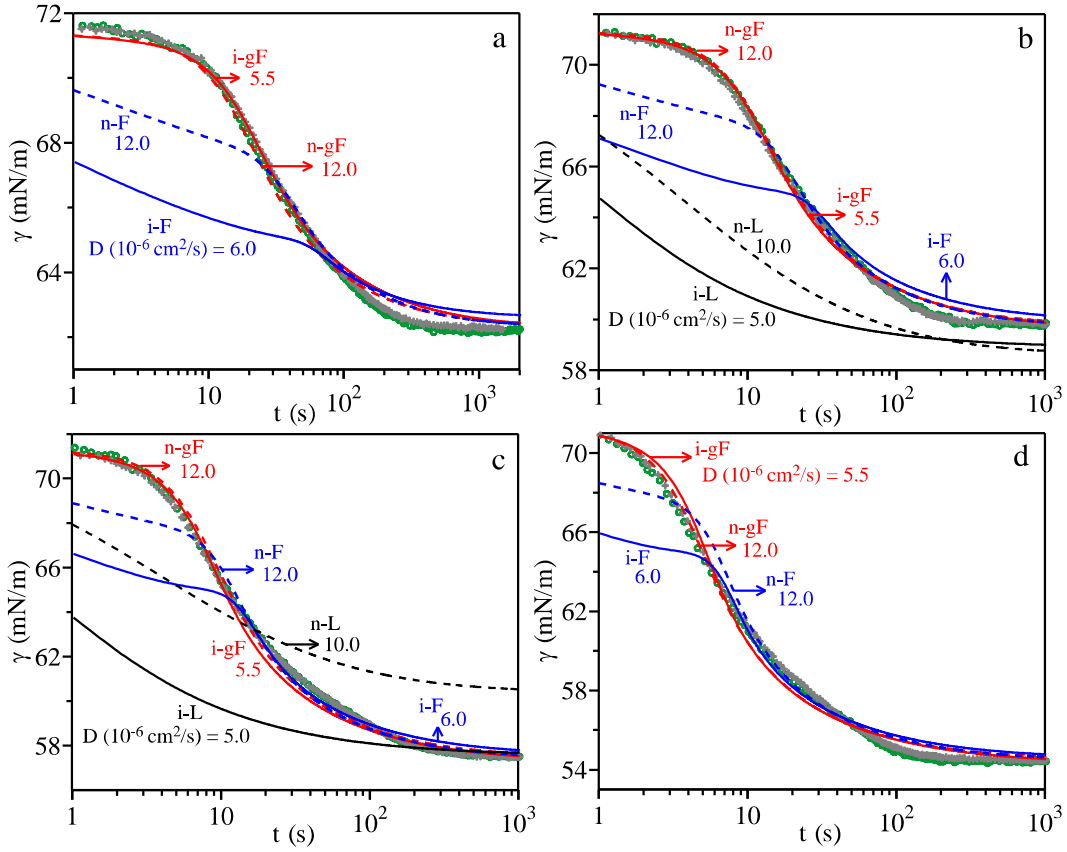

Figure 5. A comparison between the experimental ST data and the theoretical diffusion controlled ST prediction using nonionic models (dashed curves: Langmuir, Frumkin and generalized-Frumkin) and ionic models (solid curves: Langmuir, Frumkin and generalized-Frumkin) for decanoic acid aqueous solutions for C =5.0 (a), 6.0 (b), 7.0 (c) and 8.5 (d) (10^{-8} mol/cm^3).

Diffusivity. The best fit between the dynamic ST data at six different concentrations, C = 5.0–12.0 (10^{-8} mol/cm^3), and the theoretical predictions from the ionic generalized Frumkin model resulted in a unique diffusivity (i.e., 5.5×10^{-6} cm^2/s). A value of 12.0×10^{-6} cm^2/s was obtained when the nonionic generalized Frumkin model was applied at four different concentrations, C = 5.0–8.5 (10^{-8} mol/cm^3).

The value for diffusivity can be estimated from the well-known Stokes-Einstein equation [38]: $D_{AB} = K_BT/(6\pi R_A\mu_B)$, where D_{AB} is the diffusivity of solute A in the bulk phase of solvent B, K_B is Boltzmann's constant, μ_B is the viscosity of the solvent and R_A is the radius of solute. A value of $D_{AB} = 5.0\times10^{-6}$ cm^2/s for decanoic acid at 25°C is obtained from the Stokes-Einstein equation with the assumption that the solute is a sphere.

The Wilke-Chang equation [38] is also widely used to estimate molecular diffusivity in dilute solutions of non-dissociating solutes: $D_{AB} = 7.4\times10^{-9}\ T(\varphi_B M_B)^{1/2}/(\mu_B V_A^{0.6})$. Here, φ_B is the association parameter, which equals 2.6 for water, M_B is the molecular weight of the solvent, and V_A is the molar volume of solute. A diffusivity of 6.2×10^{-6} cm^2/s was obtained for decanoic acid from this equation.

The diffusivity of 5.5×10^{-6} cm^2/s from the dynamic surface tension and the ionic generalized Frumkin model for decanoic acid is very close to the predictions of the Stokes-Einstein and Wilke-Chang equations. It is noted that the diffusivity obtained from the ionic Frumkin model (6.0×10^{-6} cm^2/s) is nearly identical to that obtained from the ionic generalized Frumkin model. The nonionic Frumkin model gave a diffusivity of 12.0×10^{-6} cm^2/s, which is identical to that obtained from the nonionic generalized Frumkin model.

Surface potential. For a diffusion-controlled adsorption process, equations 3, 8 and 13 were solved simultaneously to determine the dynamic quantities $\gamma(t)$, $\Gamma(t)$, $C_s(t)$ [or $C_{1s}(t)$, $C_{1\infty}(t)$ for ionic models], and the surface potential $\psi_s(t)$. An illustration of the relaxation of these three surface properties and sub-surface concentration is plotted in Figure 6 for the case of $C=8.5\times10^{-8}$ mol/cm^3.

In the beginning of the surfactant adsorption process, surfactant molecules begin to adsorb onto the interface, and Γ and C_s begin to increase from a value of zero; at this time, the surface charge density quickly increases (i.e., a large increase in the surface electrical potential $-\psi_s$). Essentially, the surface potential ψ_s reaches its minimum when the surface tension reaches its maximum decreasing rate ($-d\gamma/dt$). Subsequently, the surface potential becomes slightly less strong, and then

levels off when ST and the surface concentration approach their equilibrium values. It is noteworthy that the relaxation of the sub-surface concentration (C_{1s}) predicted by the ionic generalized Frumkin model is very close to that (C_s) predicted by the nonionic generalized Frumkin model.

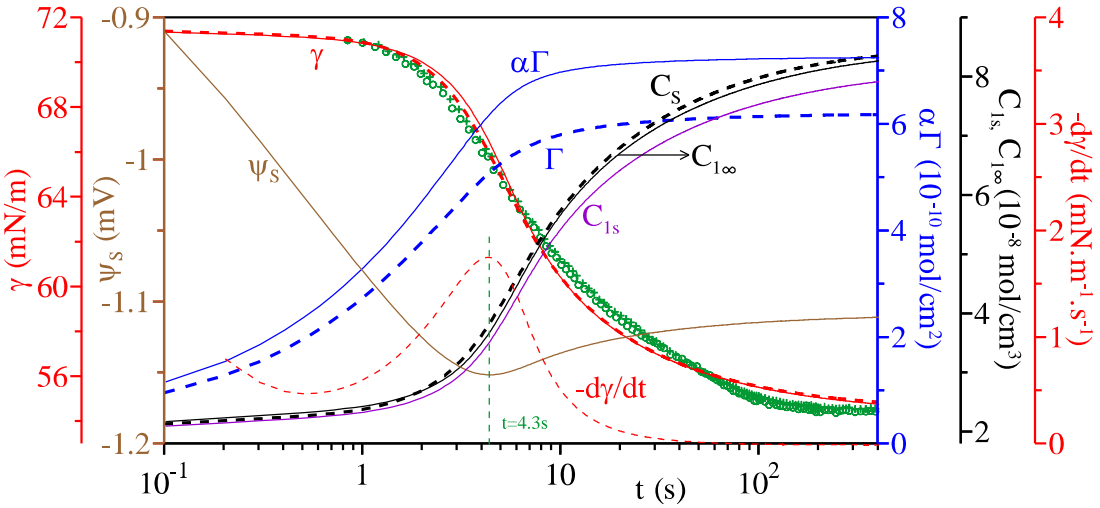

Figure 6. Relaxations of the surface properties (γ, αΓ, ψ_s and dγ/dt) predicted by the ionic generalized Frumkin (solid curves) model for C = 8.5×10^{-8} mol/cm^3. The dashed curves show the γ, Γ, and C_s values predicted by the nonionic generalized Frumkin model. The relaxations of the surfactant concentration at the subsurface (C_{1s}) and outer double layer ($C_{1\infty}$) are given for comparison.

A minimum surface potential (−1.15 mV) on the ψ_s relaxation curve exists only when the surfactant concentration is > 4×10^{-8} mol/cm^3. Figure 7 indicates that $-\psi_s$ increases monotonically for C < 4×10^{-8} mol/cm^3 during the adsorption process and reaches an equilibrium value. This equilibrium surface potential becomes stronger at higher surfactant concentrations until the bulk concentration reaches 4×10^{-8} mol/cm^3. It is notable that there exists a fixed minimum ψ_s when the surfactant concentration is larger than 4×10^{-8} mol/cm^3. This minimum ψ_s value is dependent upon the model used (F or gF; a weak dependence) and the set of model parameters (Γ_∞, a, K and n; dependent upon the equilibrium γ(C) data). The equilibrium surface potential ψ_s becomes weaker when the adsorption process proceeds further and reaches equilibrium (as shown in Figure 7) for C > 4×10^{-8} mol/cm^3. Notably, no such minimum ψ_s phenomenon occurs when a significant concentration of salt was added into the surfactant solution.

In the beginning of the adsorption process, the surface charge density begins to build up at the air-water interface. The electric potential distribution inside the electric double layer can be described by the Poisson-Boltzmann equation (eq. 10). Equation 10 can be integrated with the

boundary condition $\Psi(r=b)=\Psi_s$ to give the $\Psi(r)$ relation:

$$\psi=\frac{4RT}{z_1F}\tanh^{-1}\left\{\exp\left(\frac{z_1F}{RT}\left(\frac{RT}{\varepsilon}\sum_i C_{i\infty}\right)^{1/2}(r-b)\right)\tanh\left(\frac{z_1F\psi_S}{4RT}\right)\right\} \qquad (16)$$

where r is the distance away from the air-water interface.

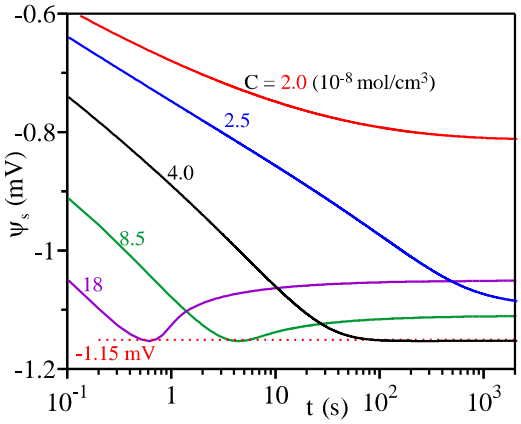

Figure 7. Relaxations of the surface potential of aqueous decanoic acid solutions predicted using the ionic generalized Frumkin model at various bulk concentrations: C = 2.0, 2.5, 4.0, 8.5, and 18 (10^{-8} mol/cm^3).

Figure 8 shows the potential distribution in the electric double layer resulted from eq. (16). The data indicate that the electric potential falls off monotonically from the surface potential (ψ_s) to the electroneutral potential ($\psi=0$) at r = λ (i.e., the electric double layer thickness where the surfactant concentration = $C_{1\infty}$). In the very early stages of the process (t < 1 s), the electrical potential $-\psi$ increases significantly with time and a nearly constant $\psi(r)$ value is observed at r<10 nm and at t < 0.001 s. The constant value of ψ becomes shorter during the course of surfactant adsorption. After a specific time (e.g., t ~ 1 s in Figure 8), this constant value disappears and a monotonically decreasing profile for $\psi(r)$ was observed. After this specific time, the distribution of $\psi(r)$ changes only slightly for 1 < t <2000 s at C = 8.5×10^{-8} mol/cm^3. This specific time t_ψ is dependent on the bulk concentration; for example, t_ψ= 10 and 0.3 s for C = 5.0 and 12.0 (10^{-8} mol/cm^3), respectively.

To describe the relaxation of the electric double layer thickness (λ) as a function of time in this surfactant adsorption process, we defined a position where $-\psi_s$ = 0.02 mV (i.e., ~2% of ψ_{max}) in the outer electric double layer (r = λ) since ψ_{max} = −1.15 mV. An illustrative example of this is shown in Figure 9 for decanoic acid solutions at C = 5.0, 8.5, and 12.0 (10^{-8} mol/cm^3). The data indicate that λ decreases dramatically during the surfactant adsorption. For example, at C = 8.5×10^{-8} mol/cm^3, λ decreases from ~650 nm to ~200 nm within 1 s, then down to ~120 nm as the adsorption approaches equilibrium.

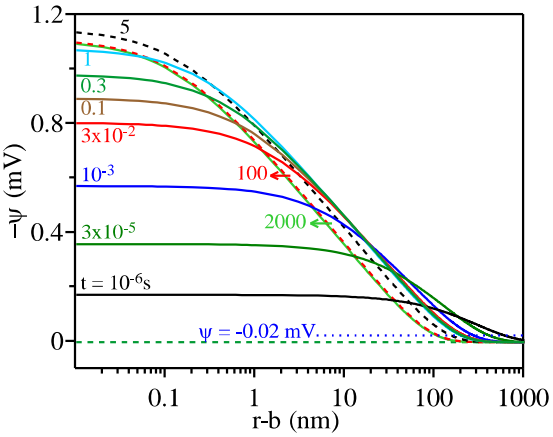

Figure 8. An illustration of the electrical potential distribution in an electric double layer at different times of the surfactant adsorption process for a decanoic acid solution at C = 8.5×10^{-8} mol/cm^3.

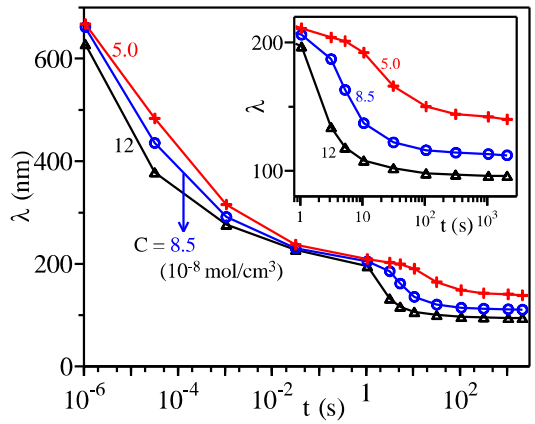

Figure 9. Relaxation of the electric double layer thickness (λ) as a function of time for decanoic acid solutions at C =5.0 (+), 8.5 (○), and 12 (Δ) (10^{-8} mol/cm^3). The inset shows the relaxation of λ at t > 1 s.

5. Discussion and Conclusions

In this study, dynamic and equilibrium surface tensions of aqueous decanoic acid solutions were measured using a pendant bubble tensiometer. The dynamic and equilibrium ST data were then compared with theoretical ST profiles simulated from both ionic and nonionic models. Both of the ionic and nonionic generalized Frumkin models predict the equilibrium surface tension well. A comparison indicated that the adsorption process is diffusion controlled, and a diffusivity of 5.5×10^{-6} cm^2/s was determined using the ionic generalized Frumkin model. Relaxation of the surface properties (Γ and ψ_s), subsurface concentrations (C_{1s} and $C_{1\infty}$), electrical potential ψ(r), and electric double layer thickness λ(t) was reported.

For an ionic surfactant, information on the dissociation degree α is required when one applies the Gibbs adsorption equation, $d\gamma = -\alpha\Gamma RT\, d\ln C$, to calculate a reduction of the surface tension. It is

widely accepted that $\alpha = 1$ for non-ionic surfactants and $\alpha = 2$ for fully dissociated ionic surfactants like SDS (Sodium Dodecyl Sulfate). When decanoic acid molecules are dissolved in water, only some of the molecules become dissociated. Therefore, the dissociation degree is concentration dependent for decanoic acid in this study, and $1 < \alpha < 2$ because of its partial dissociation.

In this work, the pH value was measured for different surfactant concentrations. Figure 10 shows the effect of concentration on pH and dissociation degree of aqueous decanoic acid solutions. The dissociation degree decreases nearly linearly at low concentration in the range 40–80%. At higher concentrations, the dissociation degree decreases slowly and approaches ~30%. However, the dissociation does not affect the calculation of the surface tension reduction following surfactant adsorption since $\alpha\Gamma_\infty$ behaves as one parameter (Table 1).

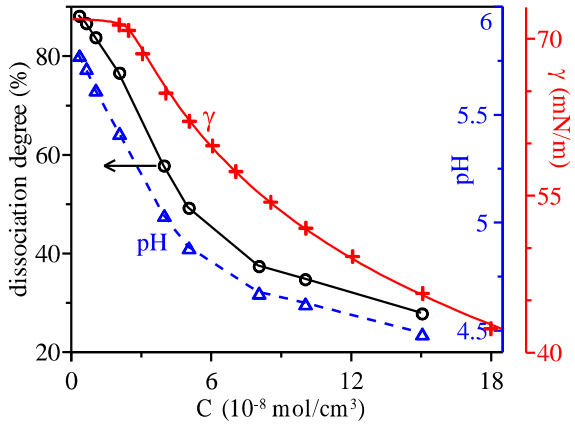

Figure 10. The effect of concentration on pH, dissociation degree, and surface tension for aqueous decanoic acid solutions.

It has been reported in ref [39] that there exists a critical K value (one of the three model parameters in the Frumkin isotherm) for nonionic surfactants in which a phase transition (i.e., the gaseous and liquid phases co-exist at the air-water interface) occurs. This critical value is $K_c = 4$ for the Frumkin isotherm and is dependent on the model parameter n when the generalized Frumkin isotherm is used (i.e., $K_c = -(1+1/n)^{1+n}$).

For an ionic surfactant, eqs. 13 and 15 can be used to determine this critical K value. Figure 11a shows an illustration of the π–A relationship for the Frumkin isotherm (n = 1), in which $K_c = -7.464$. The values of K_c at other n values are shown in Figure11b. In this study, $K_c = -27.72$ for decanoic acid when using the i-gF model with n = 0.138.

Figure 12a shows the dependence between the electrical equilibrium surface potential ψ_s and the surfactant concentration for an aqueous decanoic acid solution based on the ionic generalized Frumkin isothem. The data indicate that the surface charge density increases quickly at dilute

surfactant concentrations, where the surface pressure $\pi < 1$ mN/m and the surface coverage $x < 0.25$. The surface potential ψ_s becomes stronger when more surfactant molecules adsorb onto the air-water interface, and it reaches a maximum $-\psi_s$ (1.15 mV) at $\pi \sim 6.5$ mN/m with a surface coverage $x \sim 0.85$. ψ_s becomes slightly less negative when the surface coverage becomes more saturated ($x>0.85$).

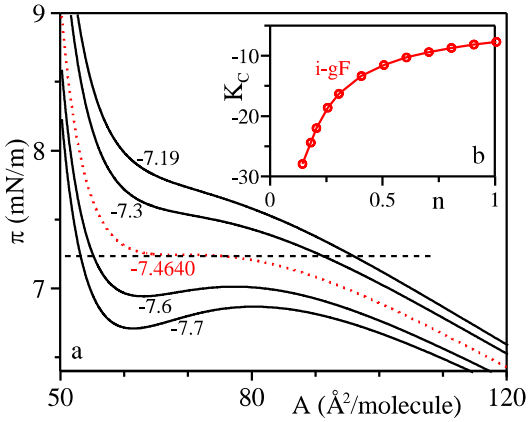

Figure 11. (a) The π–A relationship for the Frumkin isotherm. The π–A curve with a zero slope indicates the coexistence of gaseous and liquid phases at the air-water interface (i.e., the occurrence of a phase transition). (b) The dependence of model parameter n on the critical K value.

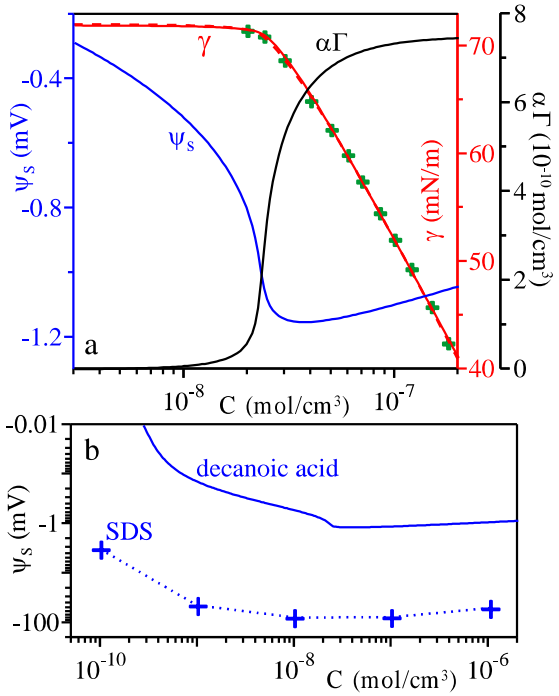

Figure 12. (a) The dependence between the surface potential ψ_s (calculated using the ionic generalized Frumkin model) and the surfactant concentration for an aqueous decanoic acid solution. (b) A comparison of the surface potentials ψ_s of aqueous SDS (ref. 40) and decanoic acid (this study) solutions.

Figure 12b illustrates a comparison of the electrical equilibrium surface potential of decanoic acid at the air-water interface in this work and that of SDS from Nakahara et al. [40] using the ionizing ^{241}Am electrode method. The data indicate that SDS has a much stronger electric charge density, with a surface potential that is nearly two orders of magnitude larger than that determined for decanoic acid.

Acknowledgements

The authors would like to express great appreciation to NSC for financial support (103-2221-E-011-158).

References

[1] P. Pomerantz, W.C. Clinton, W.A. Zisman, J. Colloid Interface Sci. 24 (1967) 16.

[2] B.E. Chistyakov, Theory and practical application aspects of surfactants, in: Surfactants Chem. Interfacial Prop. Appl., 2001: pp. 511–618.

[3] S.S. Dukhin, R. Miller, G. Kretzschmar, On the theory of adsorption kinetics of ionic surfactants at fluid interfaces, Colloid Polym. Sci. 269 (1991) 923–928.

[4] C. Tanford, The Hydrophobic Effect., John Wiley and Sons, New York, 1973

[5] S.Y. Lin, K. McKeigue, C. Maldarelli, AIChE J. 36 (1990) 1785.

[6] S.S. Datwani, K.J. Stebe, Langmuir. 17 (2001) 4287.

[7] C. Stubenrauch, V.B. Fainerman, E.V. Aksenenko, R. Miller, J. Phys. Chem. B. 109 (2005) 1505.

[8] N. Mucic, N.M. Kovalchuk, V. Pradines, A. Javadi, E.V. Aksenenko, J. Kragel, R. Miller, Colloids. Surf. A. 441 (2014) 825.

[9] Y.J. Jiang, T. Geng, Q.X. Li, G.J. Li, H.B. Ju, J. Molecular. Liq. 204 (2015) 126.

[10] F. Giusti, J.L. Popot, C. Tribet, Langmuir. 28 (2012) 10372.

[11] H. Ritacco, D. Langevin, H. Diamant, D. Andelman, Langmuir. 27 (2011) 1009.

[12] R. Jiang, Y.H. Ma, J.X. Zhao, J. Colloid. Interface. Sci. 297 (2006) 412.

[13] V.G. Babak, J. Desbrieres, Colloid. Polym. Sci. 284 (2006) 745.

[14] N. Aydogan, N.L. Abbott, Langmuir. 18 (2002) 7826.

[15] I.U. Vakarelski, C.D. Dushkin, Colloids. Surf. A. 163 (2000) 177.

[16] A.V. Makievski, R. Miller, G. Czichocki, V.B. Fainerman, Colloids. Surf. A. 133 (1998) 313.

[17] A. Bonfillon, F. Sicoli, D. Langevin, J. Colloid. Interface. Sci. 168 (1994) 497.

[18] J.T. Davies, E.K. Rideal, Interfacial Phenomena, Academic Press, New York, 1963.

[19] S.S. Dukhin, R. Miller, G. Kretzschmar, Colloid. Polym. Sci. 261 (1983) 335.

[20] R. Miller, S.S. Dukhin, G. Kretzschmar, Colloid. Polym. Sci. 263 (1985) 420.

[21] S.S. Dukhin, R. Miller, Colloid. Polym. Sci. 269 (1991) 923.

[22] G. Gouy, J. Phys. Radium (Paris). 9 (1910) 457.

[23] D.L.Chapman, Philos. Mag. 25 (1913) 475.

[24] R.P. Borwankar, D.T. Wasan, Chem. Eng. Sci. 41 (1986) 199.

[25] R.P. Borwankar, D.T. Wasan, Chem. Eng. Sci. 43 (1988) 1323.

[26] V.B. Fainerman, E.H. Lucassen-Reynders, R. Miller, Colloids. Surf. A. 143 (1998) 141.

[27] V.B. Fainerman, E.H. Lucassen-Reynders, Adv. Colloid. Interf. Sci. 96 (2002) 295.

[28] C.A. MacLeod, C.J. Radke, Langmuir. 10 (1994) 3555.

[29] A. Fick, Ann. der Physik. 94 (1885) 95-86.

[30] A.F.H. Ward, L. Tordai, J. Chem. Phys. 14 (1946) 453.

[31] E.J.Y. Verwey, J.Th.G. Overbeek, Theory of Stability of Lyophobic Colloids. Elsevier, Amsterdam, 1948.

[32] D. Myers, Surfaces, Interfaces, and Colloids: Principles and Applications 2nd edition, John Wiley and Sons, New York, 1999.

[33] S.Y. Lin, K. McKeigue, C. Maldarelli, Langmuir. 10 (1994) 3442.

[34] E.H. Reynders, M.v.d Tempel, Surface Equation of State for Adsorbed Surfactants, Gordon & Breach, New York, 1964 (volume B).

[35] K.L. Yang, S. Yiacoumi, C. Tsouris, Electrical Double-Layer Formation: Dekker Encyclopedia of Nanoscience and Nanotechnology, Marcel Dekker, New York, 2004.

[36] J. Ferri, K.J. Stebe, J. Colloid. Interface. Sci. 209 (1999) 1.

[37] K. Lunkenheimer, W. Barzyk, R. Hirte, R. Rudert, Langmuir. 19 (2003) 6140.

[38] R.B. Bird, W.E. Stewart, E.N. Lightfoot, Transport Phenomena, John Wiley and Sons, New York, 1960 (Chapter 16).

[39] S.Y. Lin, K. McKeigue, C. Maldarelli, Langmuir. 7 (1991) 1055.

[40] H. Nakahara, O. Shibata, Y. Moroi, Langmuir, 21 (2005) 9020.

Figure Caption.

1. A pendant bubble apparatus and the video image digitization equipment. A: light source; B: pinhole; C: filter; D: planoconvex lens; E: quartz sample cell and inverted needle inside thermostatic air chamber; F: objective lens; G: video camera; M: monitor; PC: personal computer; D/A: data translation card; S: syringe; SP: syringe pump; SV: solenoid valve.
2. Schematic diagram of the double-layer. λ is the characteristic length of the double-layer, C_{1s} is the surfactant concentration at the sublayer, $C_{1\infty}$ is the surfactant concentration at the outer double layer, and b is the radius of the spherical bubble.
3. Relaxations of surface tension of aqueous decanoic acid solutions at various bulk concentrations: C = 2.0 (a), 2.4 (b), 3.0 (c), 4.0 (d), 5.0 (e), 6.0 (f), 7.0 (g), 8.5 (h), 10.0 (i), 12.0 (j), 15.0 (k), and 18.0 (l) (10^{-8} mol/cm^3).
4. Equilibrium surface tension of aqueous decanoic acid solutions and the theoretical predictions of nonionic (dashed curves) and ionic (solid curves) models. Model constants are listed in Table 1.
5. A comparison between the experimental ST data and the theoretical diffusion controlled ST prediction using nonionic models (dashed curves: Langmuir, Frumkin and generalized-Frumkin) and ionic models (solid curves: Langmuir, Frumkin and generalized-Frumkin) for decanoic acid aqueous solutions for C =5.0 (a), 6.0 (b), 7.0 (c) and 8.5 (d) (10^{-8} mol/cm^3).
6. Relaxations of the surface properties (γ, $\alpha\Gamma$, ψ_s and $d\gamma/dt$) predicted by the ionic generalized Frumkin (solid curves) model for C = 8.5×10^{-8} mol/cm^3. The dashed curves show the γ, Γ, and C_s values predicted by the nonionic generalized Frumkin model. The relaxations of the surfactant concentration at the subsurface (C_{1s}) and outer double layer ($C_{1\infty}$) are given for comparison.
7. Relaxations of the surface potential of aqueous decanoic acid solutions predicted using the ionic generalized Frumkin model at various bulk concentrations: C = 2.0, 2.5, 4.0, 8.5, and 18 (10^{-8} mol/cm^3).
8. An illustration of the electrical potential distribution in an electric double layer at different times of the surfactant adsorption process for a decanoic acid solution at C = 8.5×10^{-8} mol/cm^3.
9. Relaxation of the electric double layer thickness (λ) as a function of time for decanoic acid solutions at C =5.0 (+), 8.5 ($\circ$), and 12 (Δ) (10^{-8} mol/cm^3). The inset shows the relaxation of λ at $t > 1$ s.
10. The effect of concentration on pH, dissociation degree, and surface tension for aqueous decanoic acid solutions.
11. (a) The π–A relationship for the Frumkin isotherm. The π–A curve with a zero slope indicates the coexistence of gaseous and liquid phases at the air-water interface (i.e., the occurrence of a phase transition). (b) The dependence of model parameter n on the critical K value.
12. (a) The dependence between the surface potential ψ_s (calculated using the ionic generalized Frumkin model) and the surfactant concentration for an aqueous decanoic acid solution. (b) A comparison of the surface potentials ψ_s of aqueous SDS (ref. 40) and decanoic acid (this study) solutions.

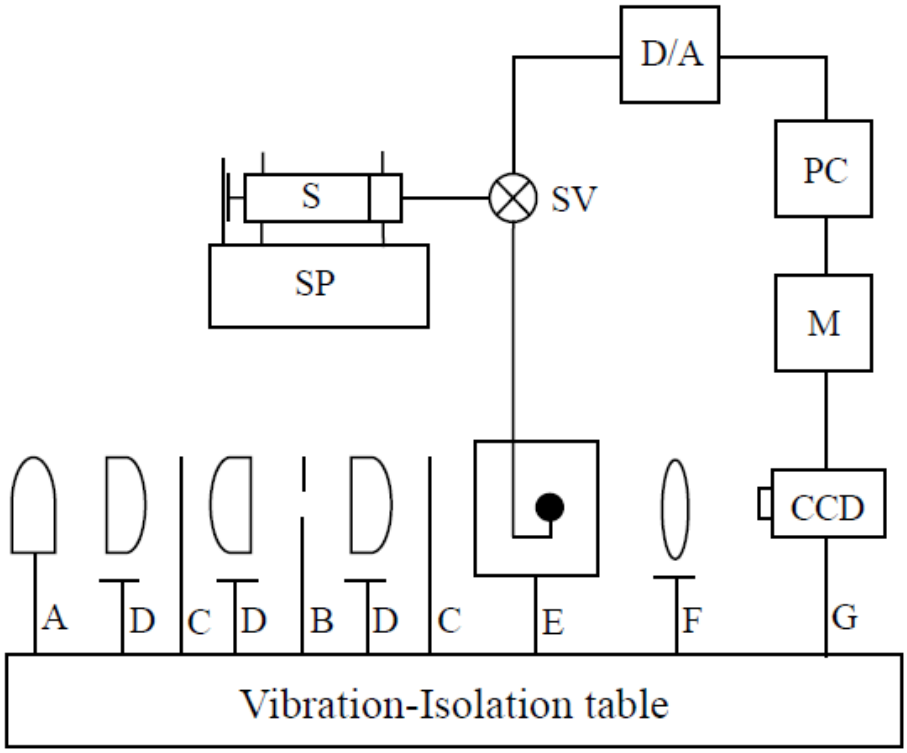
D/A
PC
S
SV
SP
M
CCD
A
D
C
D
B
D
C
E
F
G
Vibration-Isolation table

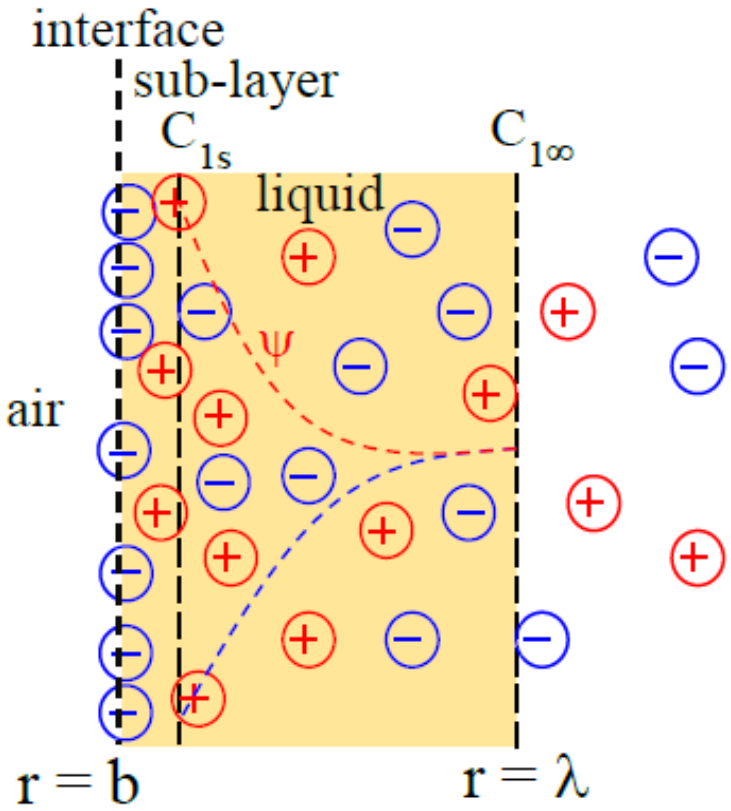
interface
sub-layer
C_{1s}
$C_{1\infty}$
liquid
ψ
air
r = b
r = λ

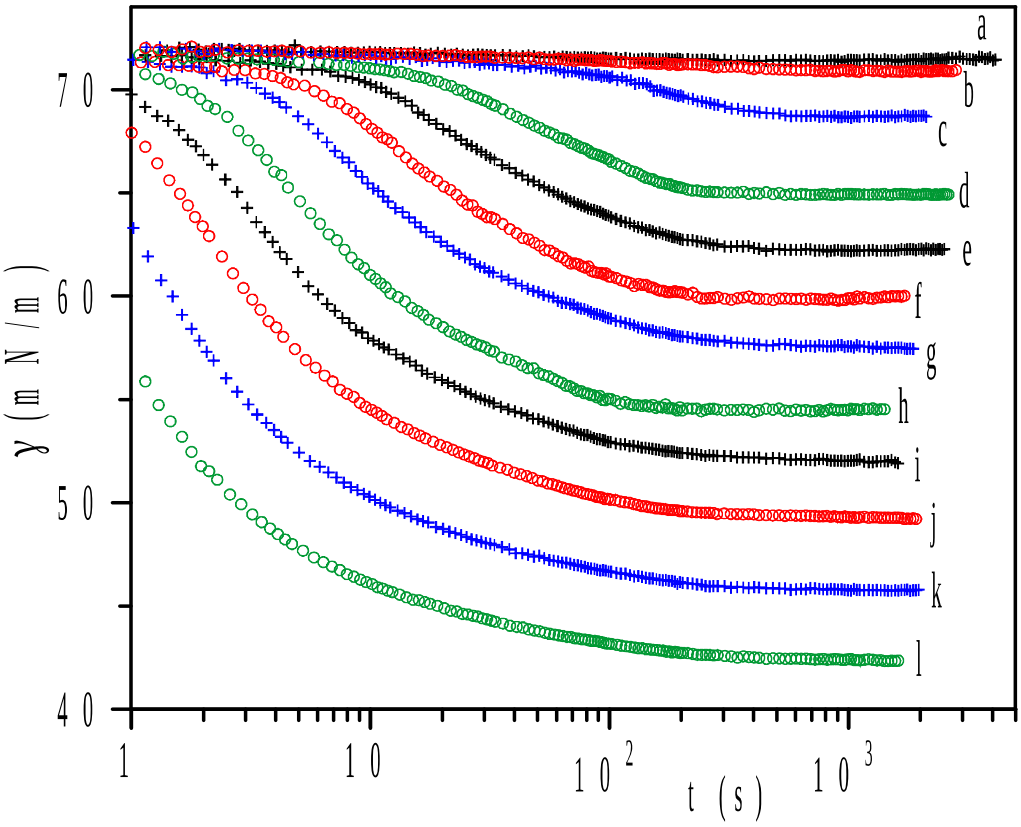
γ (mN/m)
70
60
50
40
1
10
10^2
10^3
t (s)
a
b
c
d
e
f
g
h
i
j
k
l

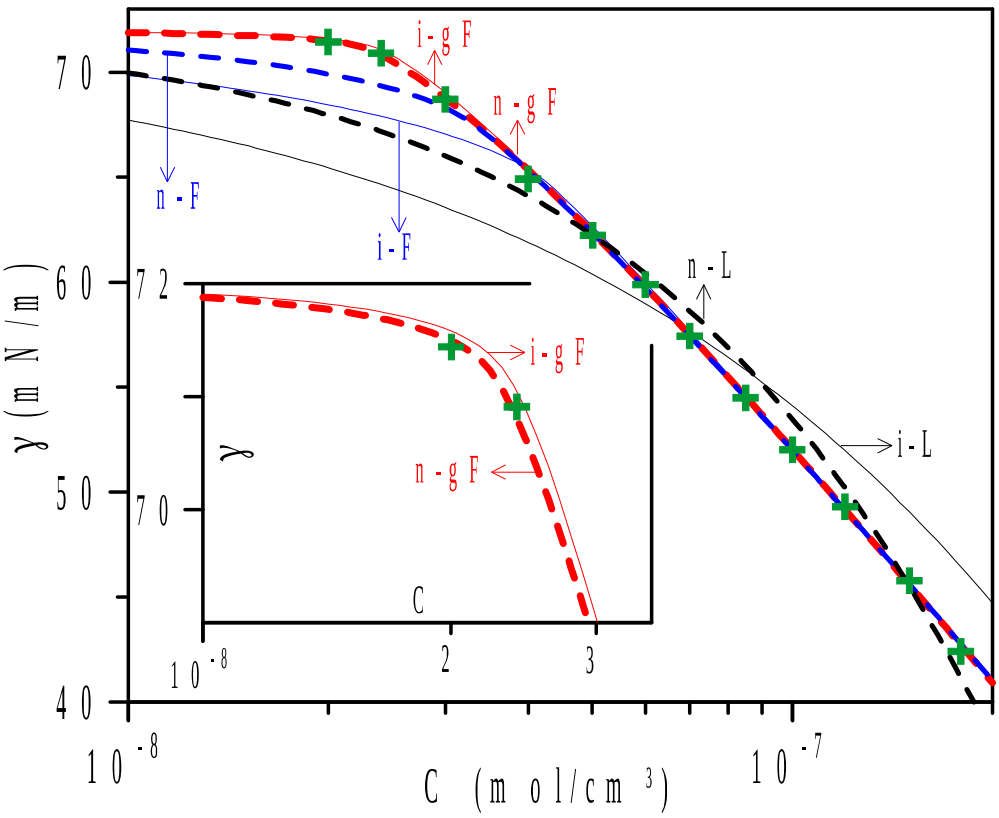
i-gF
n-gF
n-F
i-F
n-L
i-L
γ (mN/m)
70
60
50
40
10-8
C (mol/cm3)
10-7
72
70
γ
i-gF
n-gF
C
10-8
2
3

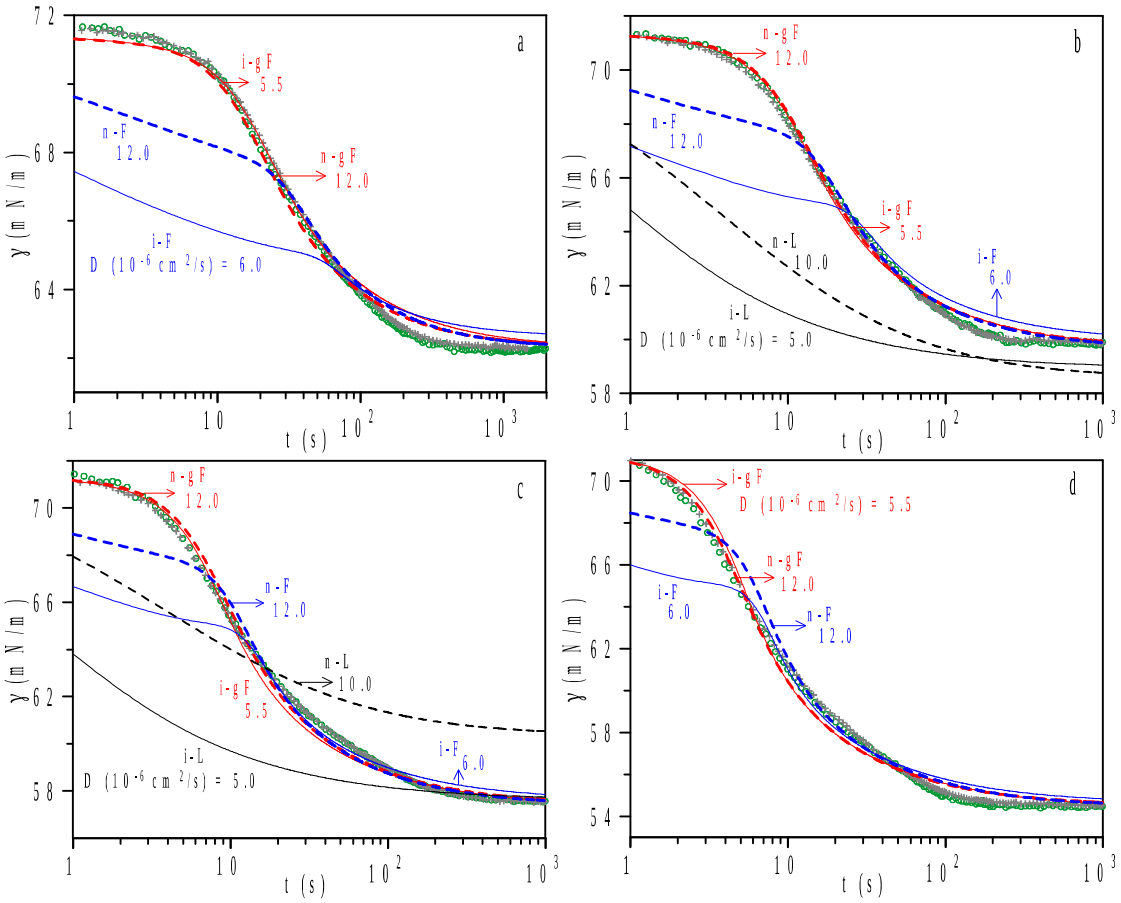
a
i-gF 5.5
n-gF 12.0
n-F 12.0
i-F D (10⁻⁶ cm²/s) = 6.0
γ (mN/m)
t (s)
b
n-gF 12.0
n-F 12.0
i-gF 5.5
n-L 10.0
i-F 6.0
i-L D (10⁻⁶ cm²/s) = 5.0
γ (mN/m)
t (s)
c
n-gF 12.0
n-F 12.0
n-L 10.0
i-gF 5.5
i-F 6.0
i-L D (10⁻⁶ cm²/s) = 5.0
γ (mN/m)
t (s)
d
i-gF D (10⁻⁶ cm²/s) = 5.5
n-gF 12.0
i-F 6.0
n-F 12.0
γ (mN/m)
t (s)

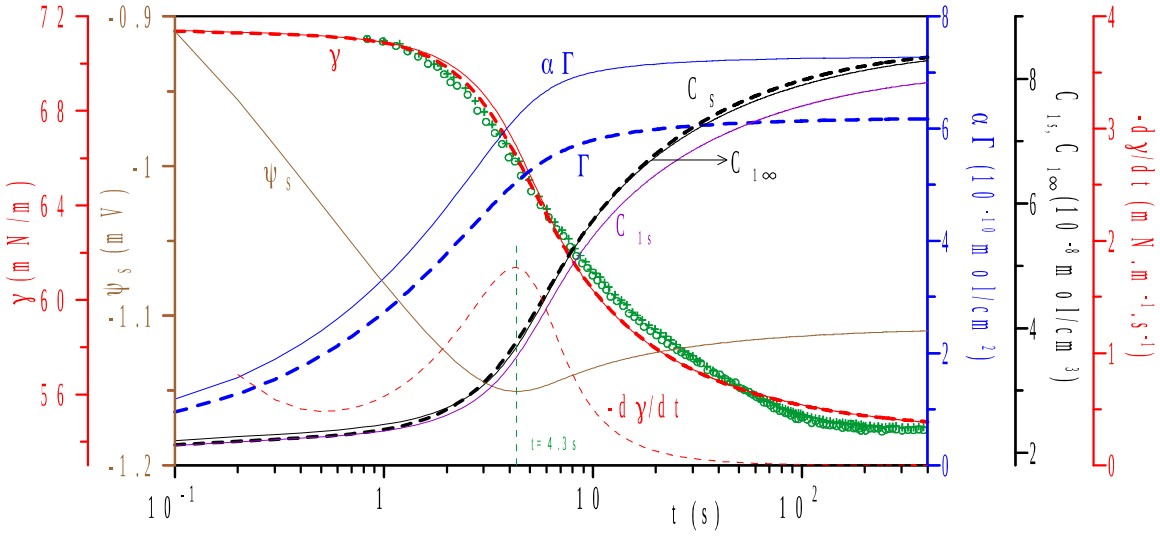
γ (mN/m)
ψ s (mV)
α Γ (10 -10 mol/cm 2)
C 1s, C 1∞ (10 -8 mol/cm 3)
-dγ/dt (mN.m -1.s -1)
γ
ψ s
α Γ
Γ
C s
C 1∞
C 1s
-d γ/d t
t= 4.3 s
t (s)
10 -1
1
10
10 2

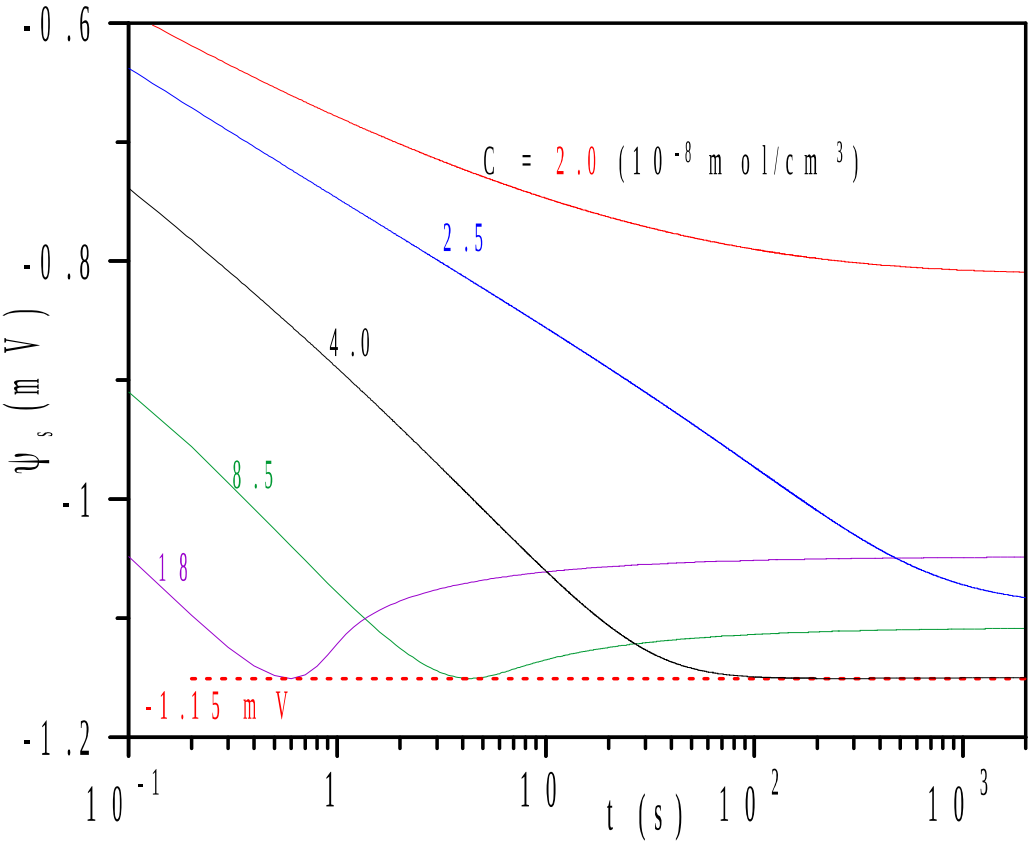
-0.6
-0.8
-1
-1.2
ψs (mV)
C = 2.0 (10-8 mol/cm3)
2.5
4.0
8.5
18
-1.15 mV
10-1
1
10
t (s)
102
103

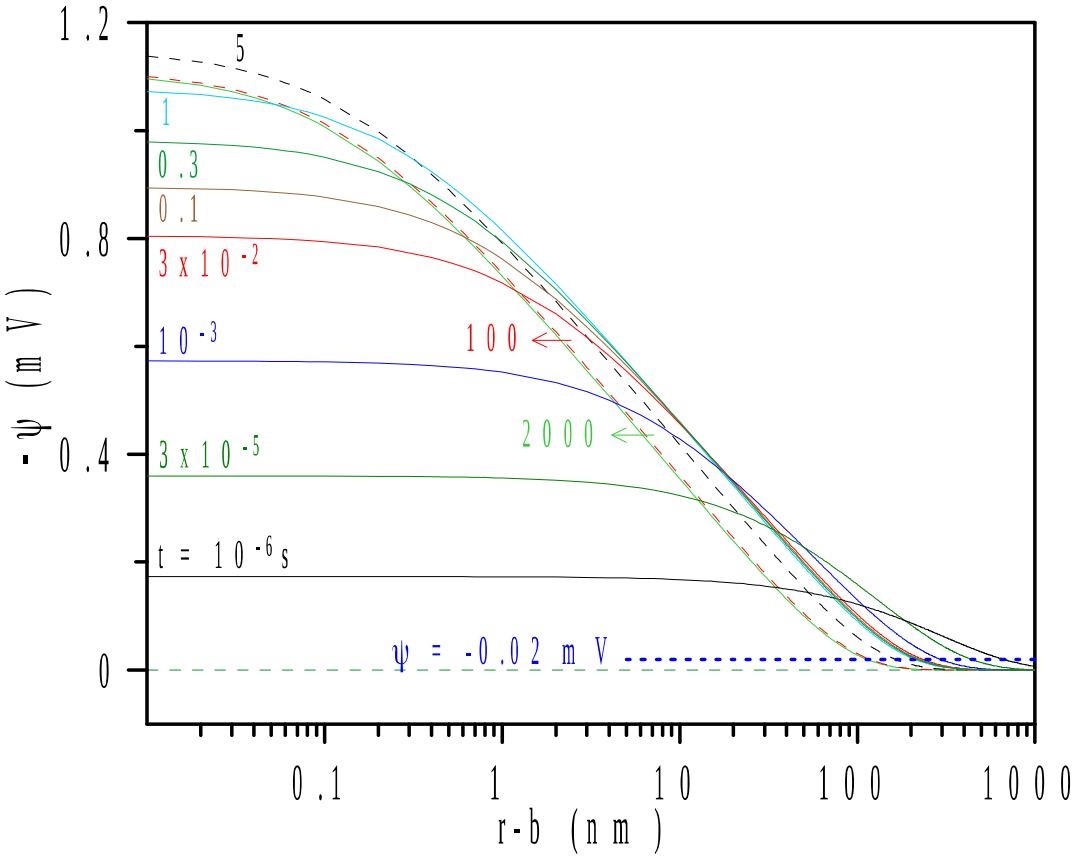
1.2
0.8
0.4
0
-ψ (mV)
5
1
0.3
0.1
3 x 10-2
10-3
3 x 10-5
t = 10-6 s
100
2000
ψ = -0.02 mV
0.1
1
10
100
1000
r-b (nm)

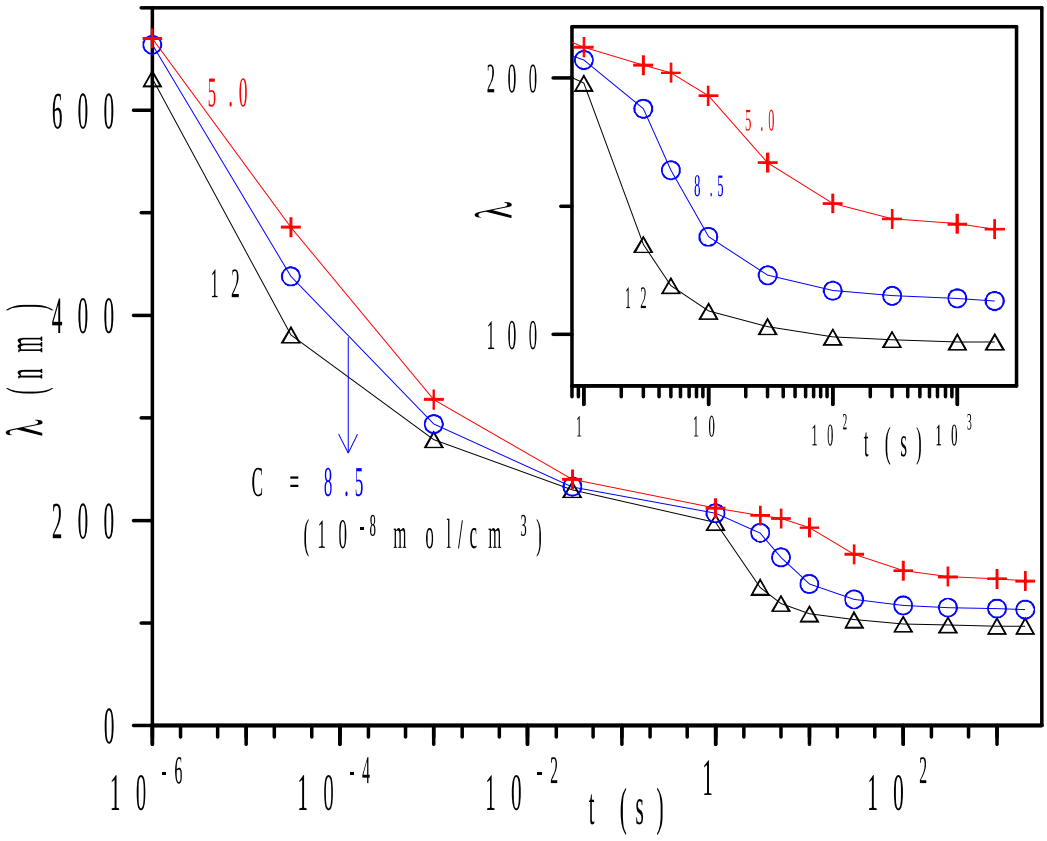
λ (nm)
600
400
200
0
10 -6
10 -4
10 -2
1
10 2
t (s)
5.0
8.5
12
C = 8.5
(10 -8 mol/cm 3)
λ
200
100
1
10
10 2
t (s)
10 3

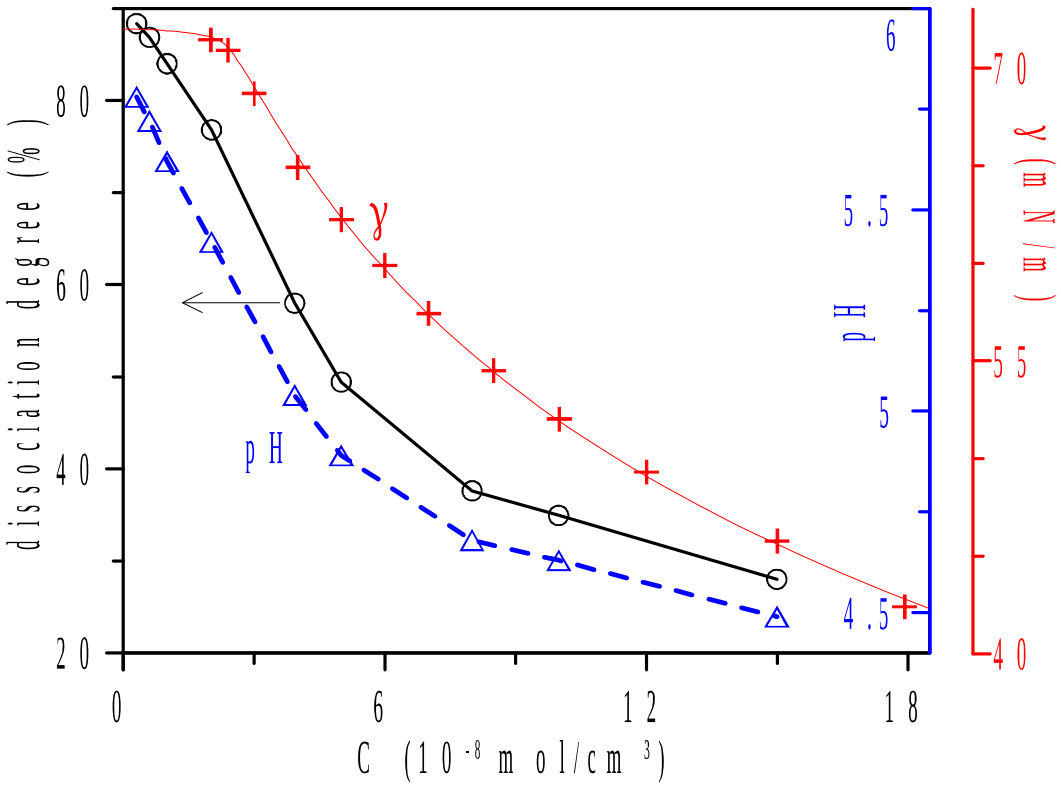
dissociation degree (%)
80
60
40
20
0
6
12
18
C (10⁻⁸ mol/cm³)
γ
pH
6
5.5
5
4.5
pH
γ (mN/m)
70
55
40

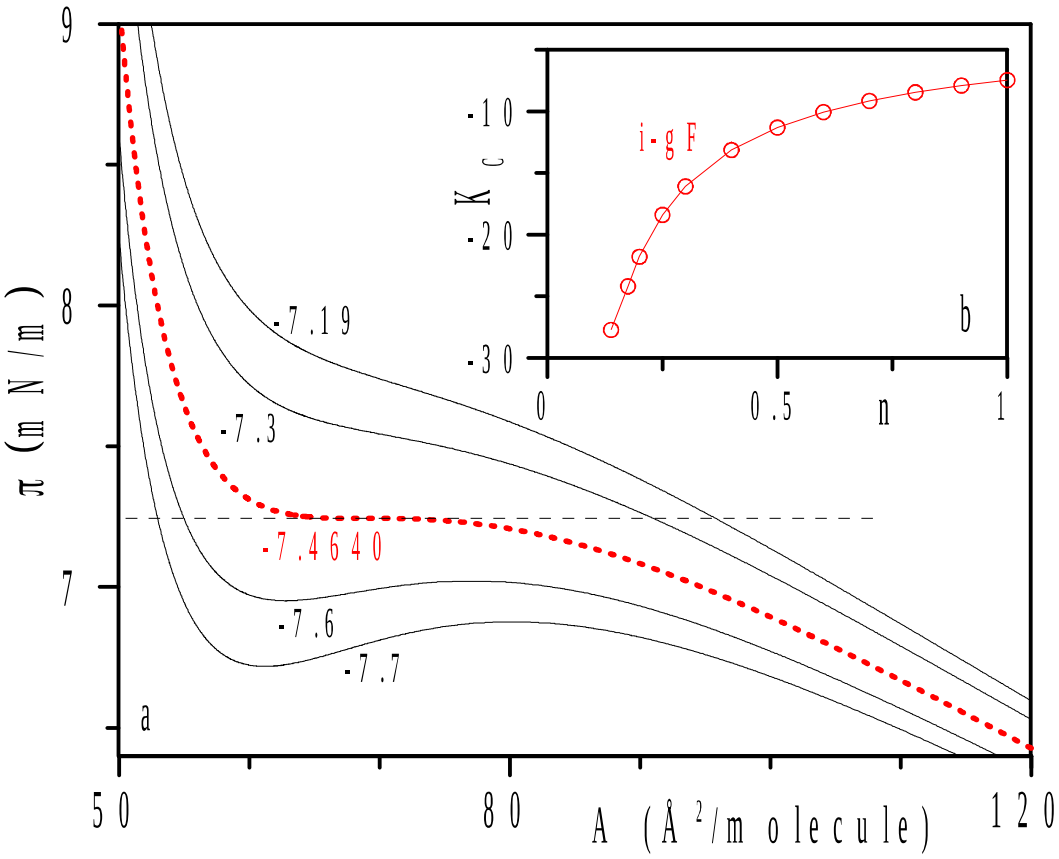
9
8
7
π (m N/m)
-7.19
-7.3
-7.4640
-7.6
-7.7
a
50
80
120
A (Å²/molecule)
-10
-20
-30
Kc
i-gF
0
0.5
n
1
b

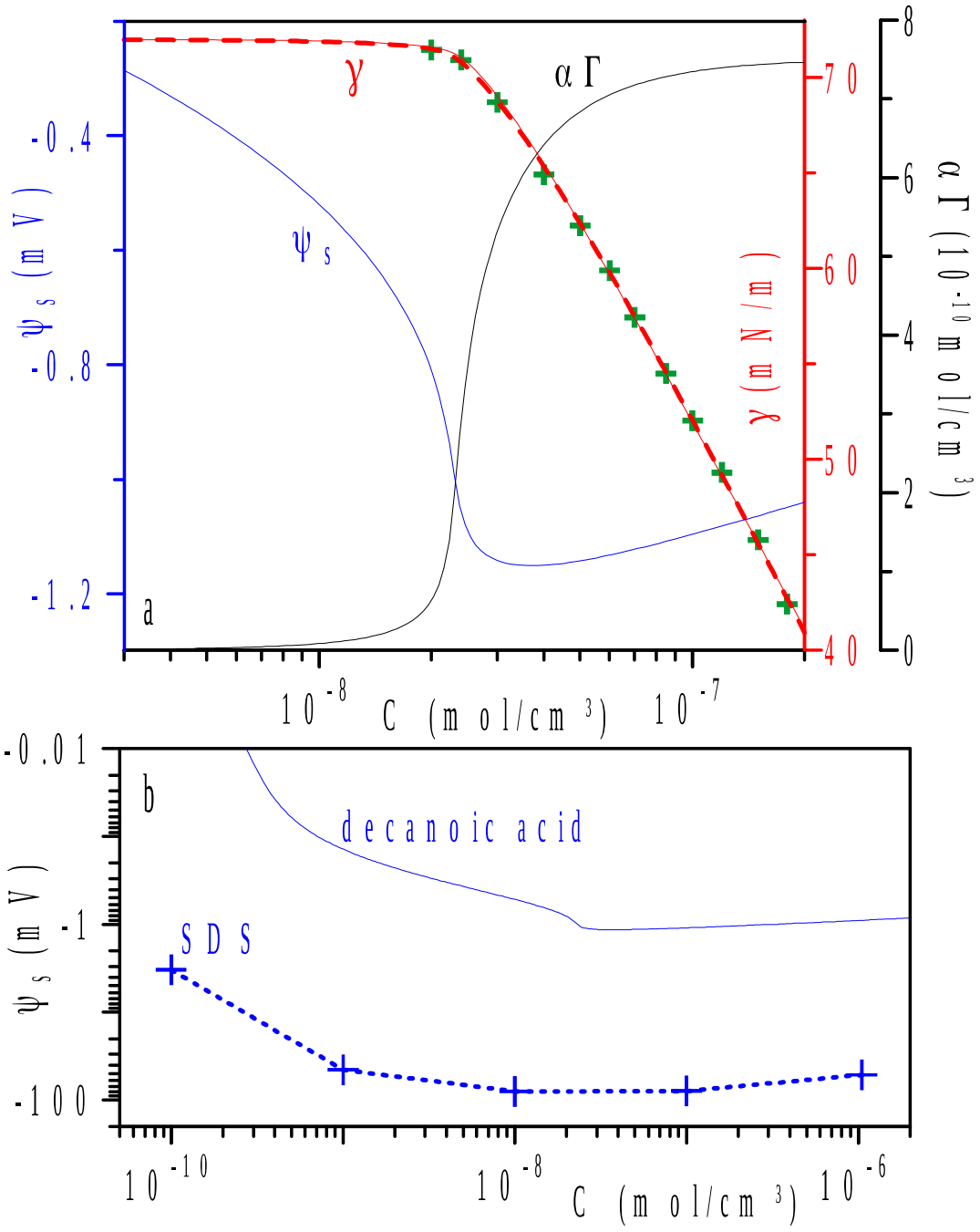
γ
α Γ
ψ s
a
-0.4
-0.8
-1.2
ψ s (m V)
70
60
50
40
γ (m N/m)
8
6
4
2
0
α Γ (10-10 m ol/cm 3)
10-8
C (m ol/cm 3)
10-7
b
-0.01
-1
-100
decanoic acid
SDS
ψ s (m V)
10-10
10-8
C (m ol/cm 3)
10-6